# Nonequilibrium Unfolding of Polyelectrolyte Condensates in Electric Fields

R. R. Netz

*Sektion Physik, LMU Munich, Theresienstrasse 37, 80333 Munich, Germany*

(Received 6 September 2002; published 28 March 2003)

Using simulations and scaling methods, the effect of an electric field on a collapsed polyelectrolyte globule is investigated, where conduction by counterions and the polyelectrolyte itself is taken into account. At a critical field $E^*$, a nonequilibrium transition occurs at which the polyelectrolyte unfolds and aligns parallel to the external field. $E^*$ is determined using scaling results for the polarizability of a polyelectrolyte globule and exhibits a dependence on the chain length $N$, $E^* \sim N^{-1/2}$, which might be useful for electrophoretic separation of charged biopolymers.

DOI: 10.1103/PhysRevLett.90.128104 PACS numbers: 87.15.He, 61.25.Hq, 82.70.–y

The behavior of polyelectrolytes (PE) exhibits a number of remarkable features which are due to the electrostatic coupling between polymeric and counterion degrees of freedom. Relevant for the present paper is the sequence of PE conformations which is observed in simulations as the electrostatic coupling between the charges on the PE and the counterions is increased [1–4]. Experimentally, the coupling can be tuned by changing temperature, dielectric constant of the solvent, counterion valency and size, or charge density of the PE. For very small coupling, the PE resembles a neutral polymer since the electrostatic repulsion between monomers is very small. As the coupling increases, the monomer-monomer repulsion leads to a more swollen configuration (the standard PE effect). However, as the coupling further increases, counterions condense on the PE, decrease the repulsion between monomers, and the PE starts to shrink. Finally, at very large electrostatic coupling, the PE is collapsed to a close-packed, almost charge-neutral condensate which contains most of its counterions. A similar sequence is experimentally seen with synthetic PEs [5] and DNA [6–9]. Of particular importance is the condensation of single DNA molecules [6,9], since comparison with simulations of single PEs is possible.

All these phenomena concern the static, equilibrium behavior of PEs. In electrophoretic experiments, PEs are subject to external electric fields and the resulting mobility is measured [10,11]. Such techniques are widely used to separate DNA and charged proteins according to their molecular weight. In these situations, the electric field induces motion of ions and PEs, thus dissipation of energy, and one is facing a nonequilibrium problem. In this paper, we study the effects of electric fields on PE condensates using dynamical simulations and scaling arguments. In contrast to previous theories, where the counterions are not taken into account explicitly [12,13] or their coupling to the PE is rather weak [14,15], we start from a strongly coupled (collapsed) PE-counterion system and investigate the resultant effects for large electric fields (i.e., far from equilibrium).

We first analyze the static (zero-field) case and develop scaling arguments for the condensation of counterions and for the polarizability of a PE globule. Our simulations show that linear-response theory describes the induced dipole moment of a condensed PE globule in an electric field quantitatively up to a critical field strength at which the PE unfolds and orients in the direction of the field. This nonequilibrium unfolding transition occurs at a polarization energy equivalent to approximately thermal energy, which, together with our estimate of the polarizability of a PE globule, shows that the critical field strength scales as $N^{-1/2}$ with the polymer length $N$. Since the PE mobility is expected to change drastically at the unfolding transition, this transition should be detectable by mobility measurements and in turn could be used for efficient separation of PEs of different length.

In our dynamic simulations, we consider a single PE chain consisting of $N$ charged beads of valency $q$ and radius $a$, in a cubic periodic box of length $D$ together with $N$ oppositely charged counterions of the same valency and radius. The box volume $D^3$ corresponds to the inverse PE concentration and plays an important role. We use the position Langevin equation, from which the velocity of the $i$th particle at time $t$ follows as

$$\dot{\mathbf{r}}_i(t) = -\mu_0 \nabla_{\mathbf{r}_i} U(t) + \mu_0 q e s_i \mathbf{E} + \boldsymbol{\xi}_i(t), \qquad (1)$$

where $\mu_0$ is the bare particle mobility, $U$ is the potential energy, $\mathbf{E}$ the external electric field, $s_i = \pm 1$ for monomers/counterions, and $\boldsymbol{\xi}_i$ is a vectorial random force acting on particle $i$. At the present stage of our theory, we neglect hydrodynamic interactions between particles (as is justified since we are mostly interested in collapsed PEs where hydrodynamic forces are overwhelmed by electrostatic forces), and the random force is correlated according to $\langle \boldsymbol{\xi}_i(t) \cdot \boldsymbol{\xi}_j(t') \rangle = 6 k_B T \mu_0 \delta(t - t') \delta_{ij}$. In the simulations, we discretize Eq. (1) with a time step $\Delta$ and rescale all lengths by the monomer/counterion radius $a$ according to $\tilde{\mathbf{r}}_i = \mathbf{r}_i / a$. The iterative Langevin equation in terms of the discrete time variable $n = t/\Delta$ now reads

$$\tilde{\mathbf{r}}_i(n+1) = \tilde{\mathbf{r}}_i(n) - \tilde{\mu}_0 \nabla_{\tilde{\mathbf{r}}_i} \tilde{U}(n) + \tilde{\mu}_0 s_i \tilde{\mathbf{E}} + \sqrt{6 \tilde{\mu}_0} \tilde{\boldsymbol{\xi}}_i(n),$$

where $\tilde{U} = U/k_B T$ is the dimensionless potential energy, $\tilde{\mathbf{E}} = qea\mathbf{E}/k_B T$ the rescaled electric field, and the

  

rescaled random force has variance unity, $\langle \tilde{\boldsymbol{\xi}}_i(m) \times \tilde{\boldsymbol{\xi}}_j(n) \rangle = \delta_{mn}\delta_{ij}$. The only dynamic parameter remaining is the rescaled mobility $\tilde{\mu}_0 = \Delta \mu_0 k_B T/a^2$ which is the diffusion constant in units of the particle radius $a$ and time step $\Delta$. In our simulations, we chose $\tilde{\mu}_0 = 0.002$ which is a good compromise between efficiency and accuracy. The potential energy has several contributions, $\tilde{U} = \tilde{U}_c + \tilde{U}_{nn} + \tilde{U}_{\mathrm{LJ}}$. The Coulombic part is

$$\tilde{U}_c = \Xi \sum_{i<j} \frac{s_i s_j}{|\tilde{\mathbf{r}}_i - \tilde{\mathbf{r}}_j|}, \tag{2}$$

where $\Xi = q^2 \ell_B/a$ is the coupling strength and measures the ratio of the Coulomb interaction and the thermal energy at a typical distance $a$ [$\ell_B = e^2/(4\pi\varepsilon k_B T)$ is the Bjerrum length, in water, $\ell_B \approx 0.7$ nm]. The connectivity of the PE is ensured by the term

$$\tilde{U}_{nn} = K \sum_{\langle ij \rangle} (|\tilde{\mathbf{r}}_i - \tilde{\mathbf{r}}_j| - 2)^2, \tag{3}$$

where the sum runs over nearest neighbors of the PE chain only. The bond stiffness is $K = 100$ which gives a very narrow distribution of bond lengths. Finally, collapse of counterions and charged monomers is prevented by a truncated Lennard-Jones term acting between all particles in the simulation,

$$\tilde{U}_{\mathrm{LJ}} = \epsilon \sum_{i<j} \left( \frac{2^{12}}{(\tilde{\mathbf{r}}_i - \tilde{\mathbf{r}}_j)^{12}} - \frac{2^7}{(\tilde{\mathbf{r}}_i - \tilde{\mathbf{r}}_j)^6} + 1 \right), \tag{4}$$

used for separation $|\tilde{\mathbf{r}}_i - \tilde{\mathbf{r}}_j| < 2$ only with an energy parameter $\epsilon = 1$. Equilibration takes roughly $10^6$ time steps, simulations were run for at least $10^7$ time steps. In Fig. 1, we show in the top panel a few snapshots of a PE chain with $N = 50$ monomers in the absence of an external field, exhibiting the well-known initial expansion of the chain due to increasing monomer-monomer repulsion, followed by a progressive condensation of counterions on the chain and concomitant collapse of the chain as the coupling parameter $\Xi$ increases. This is reflected by the rescaled polymer radius of gyration $\tilde{R}_g = \sum_i \langle (\tilde{\mathbf{r}}_i - \tilde{\mathbf{R}}_0)^2 \rangle / N$ (where $\tilde{\mathbf{R}}_0$ is the PE center of mass and the sum runs over PE monomers only) in Fig. 1(a) which shows for the various box sizes used a maximum at $\Xi \approx 3$. The number of condensed counterions in Fig. 1(b) (a counterion is rather arbitrarily defined as condensed when its center is closer than $4a$ to any monomer center) depends weakly on the box size: The bigger the box the smaller the number of condensed counterions. The simplest approach towards counterion condensation on finite-size cylinders [16] starts with the observation that the electrostatic energy of a cylinder of length $L$, radius $a$, and linear charge density $q/2a$ is (neglecting end effects) given per unit length and in units of $k_B T$ by $w \simeq \Xi \ln(L/a)/4a$. Assuming that a fraction $x$ of counterions condenses on the cylinder, the modified electrostatic energy becomes $w \simeq (1-x)^2 \Xi \ln(L/a)/4a$. Details of the counterion distribution influence only the next-leading order and are therefore irrelevant for the present arguments. The entropy cost of confining a fraction $x$ of counterions into a cylindrical compartment of approximate volume $\approx La^2$ scales (per unit length) as $s \simeq x \ln(D^3/La^2)/a$. Minimizing the total free energy $w + s$ with respect to $x$, the fraction of condensed ions, one obtains the leading result for large $L/a$ and $D/L$:

$$x = 1 - \frac{2}{\Xi}\left(1 + \frac{3 \ln D/L}{2 \ln L/a}\right). \tag{5}$$

For infinitely long cylinders $L/a = \infty$, the exact Manning

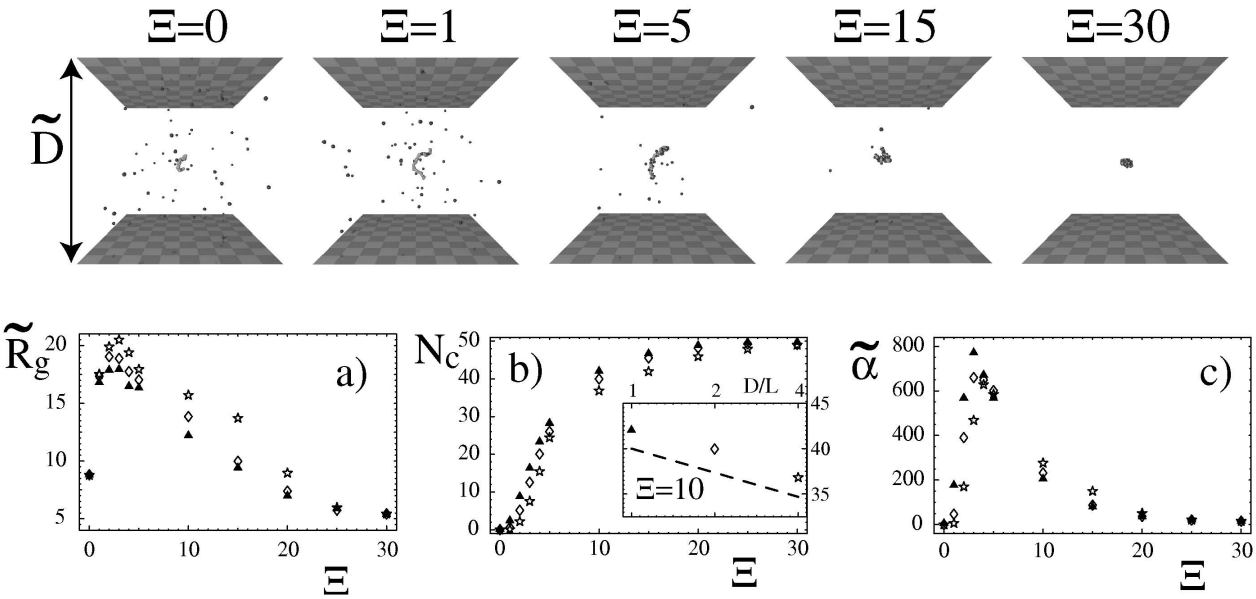


FIG. 1. Simulation snapshots of a PE with $N = 50$ monomers and approximate length $\tilde{L} \approx 100$ in a cubic box of diameter $\tilde{D} = 200$ for various values of the coupling parameter $\Xi$. (a) Radius of gyration, (b) average number of condensed counterions, and (c) polarizability for a PE of length $N = 50$ and box sizes $\tilde{D} = 400$ (stars), $\tilde{D} = 200$ (diamonds), and $\tilde{D} = 100$ (solid triangles).

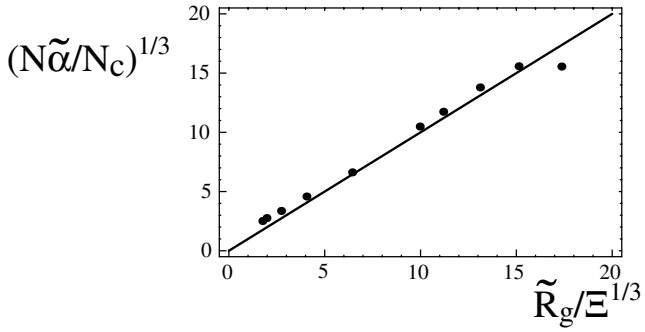


FIG. 2. Scaling plot of the polarizability for a PE with $N = 50$ monomers in a box of size $\tilde{D} = 200$, showing that $\tilde{\alpha} \simeq N_c \tilde{R}_g^3 / N\Xi$.

limit $x = 1 - 2/\Xi$ with the condensation threshold at $\Xi^* = 2$ is recovered [17], but for finite-length cylinders an increasing box size $D/L$ decreases the number of condensed ions (and in an infinite box all counterions are free). The inset of Fig. 1(b) shows numerical data for the number of condensed ions for fixed coupling strength $\Xi = 10$ together with the asymptotic prediction Eq. (5). The agreement is quite satisfactory, even though one is far from the asymptotic limit of large $L/a$ and $D/L$ and the PE is not a straight cylinder but undergoes a shape transition from a cylindrical to a spherical morphology for a characteristic value of $\Xi$ [18,19].

The rescaled dipole moment of the PE with its counterions is given by $\tilde{\mathbf{P}} = \sum_i s_i(\tilde{\mathbf{r}}_i - \tilde{\mathbf{R}}_0)$, where the sum includes only those counterions that are condensed [using the same definition as for Fig. 1(b)] on the PE. In Fig. 1(c), the polarizability according to the fluctuation-dissipation theorem, $\tilde{\alpha} = k_B T \alpha/(qea)^2 = \langle \tilde{P}^2/3 \rangle$, is shown. The classical result for the polarizability of a sphere with radius $R$ and uniformly distributed charge $Q$ around an opposite point charge $Q'$ is for $Q = Q'$ given by $\alpha = 4\pi\epsilon R^3$ [20] or, in rescaled units, $\tilde{\alpha} = \tilde{R}^3/\Xi$. Identical results are obtained from the Clausius-Mosotti equation or using different, more complicated charge distributions [19]. For a system with a net charge, $Q < Q'$, the polarizability is reduced, $\tilde{\alpha} = Q\tilde{R}^3/\Xi Q'$. Accordingly, we replot in Fig. 2 the data for $\tilde{D} = 200$ from Fig. 1(c) as $(\tilde{\alpha} N/N_c)^{1/3}$ versus $\tilde{R}_g/\Xi^{1/3}$ together with a straight line of slope unity, demonstrating that our simple scaling model allows a quantitative description of the PE polarizability [21].

Figure 3 shows a few snapshots for $\Xi = 20$ and increasing field strength, exhibiting an unfolding transition of the PE condensate at a critical field strength. The simulations are always run long enough to reach steady state and to eliminate the pronounced hysteresis effects (the time-dependent approach to steady state is currently being studied [19]). We use periodic minimal-image boundary conditions, i.e., counterions and the PE can traverse the boundaries freely, but the minimal-image conditions prevent the PE from interacting with itself. The nonequilibrium unfolding transition manifests itself as a rather abrupt increase of the rescaled end-to-end radius $\tilde{R}_e/\tilde{L}$ [see Fig. 3(a)]. The number of condensed counterions in the high-field extended configuration decreases drastically (and as a consequence the PE mobility increases [19]) as the box size becomes larger [see Fig. 3(b)]. It approximately equals the ratio of polymer length and box size, $N_c/N \approx \tilde{L}/\tilde{D}$, since the counterions are distributed almost evenly along the electric-field direction. The effective mobility of a charged particle is defined as $\tilde{\mu}_i = s_i(\tilde{\mathbf{r}}_i(n+1) - \tilde{\mathbf{r}}_i(n))/\tilde{E}$ and is equivalent to the conductivity. While the mobility of the uncondensed

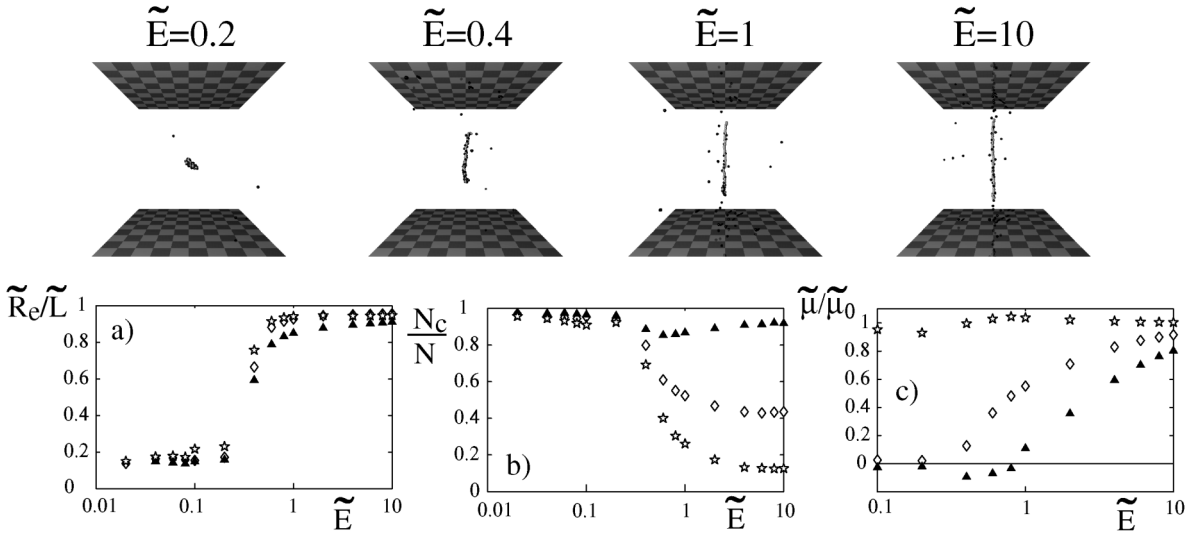


FIG. 3. PE snapshots for fixed coupling constant $\Xi = 20$ and box size $\tilde{D} = 200$ and various rescaled field strengths, exhibiting an unfolding transition at $\tilde{E} \approx 0.2$. (a) End-to-end radius $\tilde{R}_e/\tilde{L}$ and (b) number of condensed counterions $N_c/N$ for a PE of length $\tilde{L} = 100$ ($N = 50$), coupling constant $\Xi = 20$, and box sizes $\tilde{D} = 400$ (stars), $\tilde{D} = 200$ (diamonds), and $\tilde{D} = 100$ (solid triangles). (c) Mobility of condensed/uncondensed counterions (triangles/stars) and of PE monomers (diamonds) for $\tilde{D} = 200$.

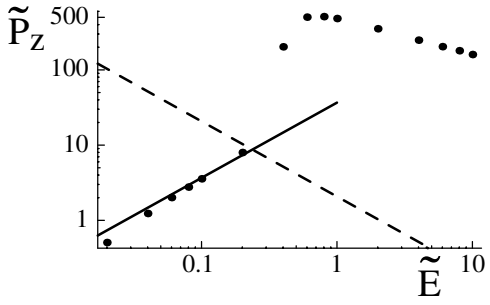


FIG. 4. Induced dipole moment $\tilde{P}_z$ for $\Xi = 20$, $\tilde{D} = 200$ as a function of the rescaled field $\tilde{E}$. The linear-response prediction, $\tilde{P} = \tilde{\alpha}\tilde{E}$ (solid line), and its limit of validity, $\tilde{P} = 2/\tilde{E}$ (broken line), are shown.

counterions is only weakly varying, the mobility of the condensed counterions and the PE monomers is small at low fields (mostly because the condensate is almost charge neutral) and reaches its maximal value slowly as the field increases [Fig. 3(c)]. Note that the bound counterion mobility is negative slightly below the unfolding threshold; counterions are dragged along with the PE in their unfavorable direction.

In Fig. 4, we plot the $z$ component of the dipole moment of the PE and its condensed counterion cloud for a box size $\tilde{D} = 200$. The solid line is the linear-response prediction $P = \alpha E$ or, in rescaled coordinates, $\tilde{P} = \tilde{\alpha}\tilde{E}$ with $\tilde{\alpha} = 36.7$ taken from the static simulation data [Fig. 1(c)]. The broken line denotes the threshold where the rescaled polarization energy $W_{\mathrm{pol}}/k_BT = PE/2k_BT = \tilde{P}\tilde{E}/2$ reaches unity, i.e., $\tilde{P} = 2/\tilde{E}$. At this threshold, the electric field is strong enough to orient the spontaneous dipole moment of the PE globule and to excite soft deformation modes: Linear-response theory is expected to break down. [Also, nonequilibrium effects are expected to be important at large electric fields. However, it is difficult to clearly separate equilibrium from nonequilibrium effects: In principle, an electric field in the absence of conduction (dissipation) would lead to similar effects, but such a scenario is impossible to study.] As the data in Figs. 3 and 4 show, this threshold indeed denotes the onset where the PE globule starts to unfold. Combining the expression for the unfolding field strength, $\tilde{E}^* = (2/\tilde{\alpha})^{1/2}$ (as follows from the condition $W_{\mathrm{pol}}/k_BT = \tilde{\alpha}\tilde{E}^2/2 = 1$), our previously demonstrated result for the polarizability of a nearly neutral globule, $\tilde{\alpha} = \tilde{R}_g^3/\Xi$, and the scaling of a compact globule, $\tilde{R}_g^3 \simeq N$, we finally obtain $\tilde{E}^* \simeq (\Xi/N)^{1/2}$, or, in nonrescaled units, $eE^* \simeq k_BT(a^3N/\ell_B)^{-1/2}$. This shows that the unfolding field strength depends on the polymer length, which could be used for electrophoretic separation studies of long PEs, which are collapsed with some condensing agent: Since the mobility is expected to change drastically with the unfolding, at a suitably chosen field strength a rather sensitive size discrimination should be possible since the longest PEs will have unfolded while the shorter ones are still collapsed.

For DNA with a linear charge density $q/2a \approx 6\ \mathrm{nm}^{-1}$, one finds $\Xi = q^2\ell_B/a \approx 8q$ and thus $\Xi \approx 24$ for trivalent counterions (e.g., spermidine). A reduced critical field, $\tilde{E}^* = 0.2$, corresponds for a particle radius $a = 0.25$ nm and trivalent ions ($q = 3$) to a field of $E \simeq 6 \times 10^6$ V/m. Extrapolating our result for $N = 50$ to longer PEs, we expect the unfolding to occur at $E \simeq 10^6$ V/m for $N = 10^3$ and $E \simeq 10^5$ V/m for $N = 10^5$ which are feasible values for capillary experiments.

Additional salt in the solution may inhibit globule formation at very large concentration; however, the mechanism for the field-induced unfolding presented here is quite insensitive to the addition of salt since the polarizability of the globule is much higher than the polarizability of the salt solution [19].

This work was financially supported by Deutsche Forschungsgemeinschaft (DFG, SFB 486) and the Fonds der Chemischen Industrie.

[1] M. Stevens and K. Kremer, Phys. Rev. Lett. **71**, 2228 (1993).
[2] R. G. Winkler, M. Gold, and P. Reineker, Phys. Rev. Lett. **80**, 3731 (1998).
[3] M. O. Khan and B. Jönsson, Biopolymers **49**, 121 (1999).
[4] S. Liu and M. Muthukumar, J. Chem. Phys. **116**, 9975 (2002).
[5] M. Olvera de la Cruz *et al.*, J. Chem. Phys. **103**, 5781 (1995).
[6] R. W. Wilson and V. A. Bloomfield, Biochemistry **18**, 2192 (1979).
[7] V. A. Bloomfield, Biopolymers **44**, 269 (1997).
[8] E. Raspaud, M. Olvera de la Cruz, J.-L. Sikorav, and F. Livolant, Biophys. J. **74**, 381 (1998).
[9] Y. Yamasaki, Y. Teramoto, and K. Yosjikawa, Biophys. J. **80**, 2823 (2001).
[10] N. C. Stellwagen, Adv. Electrophor. **1**, 177 (1987).
[11] J.-L. Viovy, Rev. Mod. Phys. **72**, 813 (2000).
[12] T. Duke and J. L. Viovy, Phys. Rev. E **49**, 2408 (1994).
[13] A. N. Semenov and J.-F. Joanny, Phys. Rev. E **55**, 789 (1997).
[14] G. S. Manning, J. Phys. Chem. **85**, 1506 (1981).
[15] D. Long, J.-L. Viovy, and A. Adjari, Phys. Rev. Lett. **76**, 3858 (1996).
[16] G. S. Manning and U. Mohanty, Physica (Amsterdam) **247A**, 196 (1997).
[17] G. S. Manning, Ber. Bunsen-Ges. Phys. Chem. **100**, 909 (1996).
[18] F. J. Solis and M. Olvera de la Cruz, J. Chem. Phys. **112**, 2030 (2000).
[19] X. Schlagberger and R. R. Netz (to be published).
[20] C. J. F. Böttcher, *Theory of Electric Polarization* (Elsevier, Amsterdam, 1973).
[21] A similar result is obtained for a PE wrapping around a sphere; see J. Dzubiella, A. G. Moreira, and P. A. Pincus (to be published).